THE 19th CHESAPEAKE SAILING YACHT SYMPOSIUM

ANNAPOLIS, MARYLAND MARCH 2009

Full Scale Measurements on a Hydrofoil International Moth

Bill Beaver, U.S. Naval Academy Hydromechanics Lab, Annapolis, MD
John Zseleczky, U.S. Naval Academy Hydromechanics Lab, Annapolis, MD

ABSTRACT

The International Moth class has experienced a resurgence of interest and publicity associated with the adoption of hydrofoils and the performance improvements these foil have brought. This paper documents a series of full scale tow tests intended to characterize some of the major parameters impacting the performance of a foiling Moth. Specifically:

- the lift and drag was measured for of various home built and commercially available T-foil configurations,
- the hydrodynamic drag of a hull was measured at various displacements, and
- the aerodynamic forces (side force and drag) were measured for a hull and racks.

It is hoped that this data will be useful for future designers to further push the state of the art.

NOMINCLATURE

β	Apparent course between V_A and V
λ	Leeway angle
ρ	Water density
AR	Aspect ratio of the lifting foil
c	Chord length of strut for lifting foil
C_{Dt}	Hoerner junction drag coefficient
C_{Dh}, C_{Lh}	Hoerner depth dependent hydrofoil drag and lift coefficients
$Cd_{induced}$	Induced drag of the lifting foil *
Cd_s	Strut section drag *
Cd_{Wave}	Lifting foil wave drag *
$Cd_{W\&S}$	Strut section wave & spray drag (normalized by t^2)
C_L	Lift coefficient of the lifting foil *
D	Drag – the horizontal force component opposite the direction of motion
h	Depth of the lifting foil from the free surface
L	Lift - the vertical force component supporting boat weight
q	Dynamic pressure ($\frac{1}{2} \rho V^2$)
Rn	Reynolds number
S	Planform area of foil
Side F	The horizontal aerodynamic side force perpendicular to the direction of motion
Strut	The vertical foil (either daggerboard or rudder)
t	Thickness of the strut or lifting foil
T-Foil	Combination of a strut and horizontal lifting foil
V	Full scale velocity
V_A	Apparent wind velocity
	* normalized by planform area

INTRODUCTION

The International Moth is a development class single-handed dingy first conceived around 1930. The Moth class rule specifies a maximum length, beam, sail area, and little else. As a result, the Moth has evolved from a conventional dinghy through scow shapes, progressively narrower skiffs with hiking wings, to now a hydrofoil supported craft. The rigs have pioneered the use of full batten sails and sleeve luffs, while the absence of a weight limit has put the Moth in the forefront of the use of carbon fiber and lightweight construction techniques. The result is an 11 foot long sailing dinghy that is part rocket ship and part water toy that brings together an eclectic group of sailors ranging from California surf kids to aerospace engineers. The performance potential of a foiler Moth is truly stunning. They require about 8 knots of wind to get up on foils, but once foil borne boat speed rarely drops below wind speed. In the right hands they are a match for any dinghy in the world, with maximum recorded speeds nearing 30 knots. Although a Moth is more difficult to sail than a conventional singlehander like a Laser, it is common for an experienced sailor to climb on and become foilborne their first time out.

The current configuration of an International Moth is a narrow hull with hiking racks supported by lifting hydrofoils under the daggerboard and rudder. The daggerboard lifting foil typically has a trailing edge flap that is activated by a surface sensing wand at the bow to provide altitude control. Additionally the angle of attack of the rudder lifting foil can be varied by twisting the tiller extension. Most foiler Moths are professionally built, but there is a dedicated contingent who design, build and sail their own boats. The boat tested for this paper, the "Hungry Beaver", was designed and built by the author. The name reflects the design linage from Marke Thorpe's "Hungry Tiger", which heavily influenced the hull design. The three areas we investigate in this paper are the hydrodynamic characteristics of the hull, the efficiency of the hydrofoils, and the aerodynamic characteristics of the hull. Ideally the characteristics of the rig would also be considered, but this is beyond the expertise of the authors and is best left for more qualified individuals.

The authors have the good fortune to work day-jobs at one of the leading tow tank testing facilities in the U.S., and have been graciously allowed to use the facilities in the off-hours to collect full scale data pertinent to Moth class boats. This project is being run in conjunction with an ongoing student hydrofoil research project and the results are intended to be useful for both endeavors.

HULL HYDRODYNAMICS

Obviously the hydrodynamic characteristics of the hull form matter far less for a Moth than just about any other sailboat, but they are not completely insignificant. Light air races are won by the ability to get on foils first and stay flying. Certainly technique is paramount, but for those of us lacking technique, any advantage wrenched from a slippery hull shape is welcome. With this in mind, the hull shape of the Hungry Beaver (HB) design is very similar to the "Hungry Tiger", which was widely regarded as the best of the pre-foilers. The hull lines of the Hungry Beaver are in Figure 1. Station lines are on 1 foot centers, buttock lines on 2 inch centers and waterlines on 4 inch centers. At the design displacement of 240 lbs, the area curve and hydrostatic characteristics are in Figure 2.

It can be stated with certainty that at some point the Hungry Beaver has sailed in the design condition (240 lbs displacement supported by buoyancy, even keel, and no roll), but only briefly. With the crew weight approaching 2.5-3 times the weight of the boat, foil lift varying with speed, roll and trim rarely being constant for more than a few seconds, the question of what to test rears its ugly head. Falling back on our mantra of simple is better (or is at least achievable), we elected to benchmark the hullform drag at 4 displacements ranging from 60 to 240 lbs while holding the LCG constant. Tests were conducted with the hull free to heave and pitch, but locked in roll and at a zero yaw angle. Resistance, pitch and heave were measured for a speed range between 2 and 14 fps. The heavy displacement is most realistic for the low speed data, while at higher speeds the foil lift unloads the hull and makes the lighter displacement data more appropriate. For speed above 14 fps (8 knots) the boat should be fully foilborne.

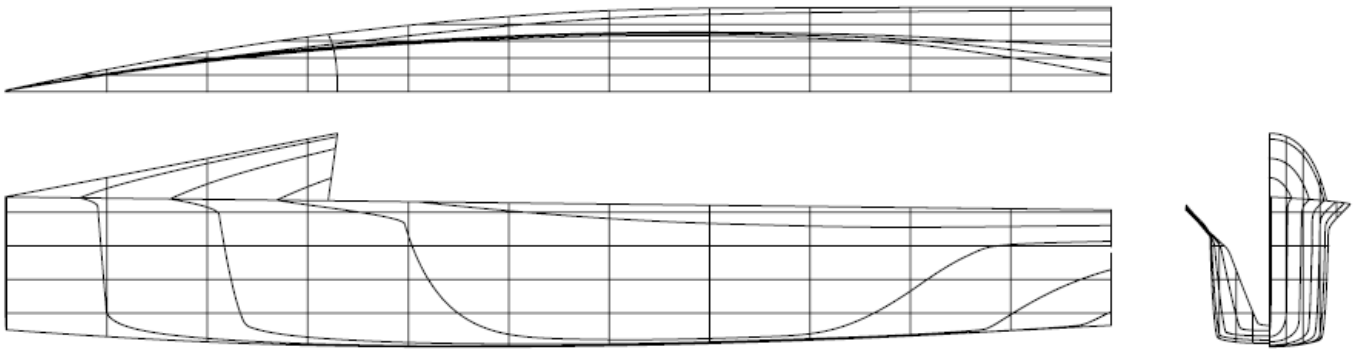

Figure 1 – Hull Lines of the Hungry Beaver

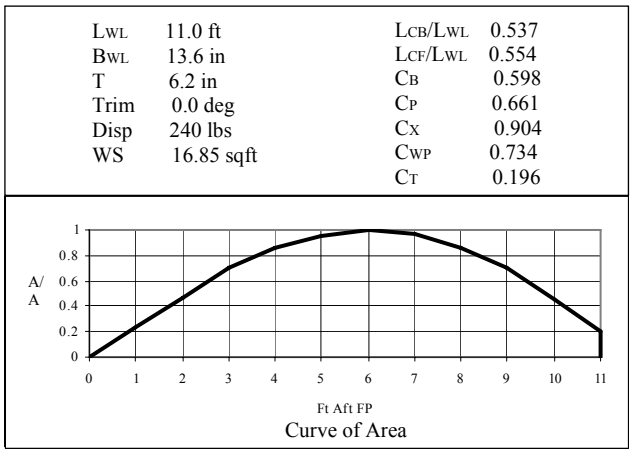

Figure 2 – Hydrostatic Characteristics of the Hungry Beaver

The resistance tests were conducted with USNA's standard surface ship tow rig, consisting of a heave post, block gage and pitch pivot. Yaw restraint was provided by a vertical rod mounted near the stern constrained by longitudinal rollers on the carriage. The tow gear was affixed to transverse strongbacks which were in turn lashed to the gunnels of the boat. A photograph and diagram of the tow rig is shown in figures 3 and 4.

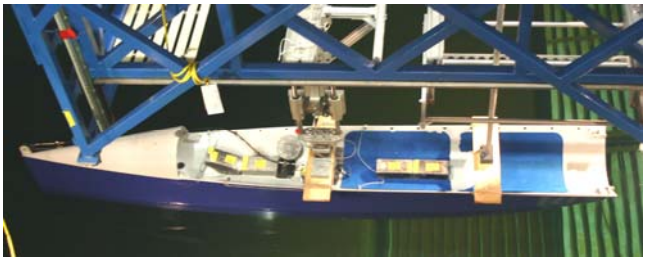

Figure 3 –Calm Water Resistance Towing Rig

The accuracy typically expected from this gear is on the order of 1.5 % while the repeatability for back-to-back tests is about 0.5%.

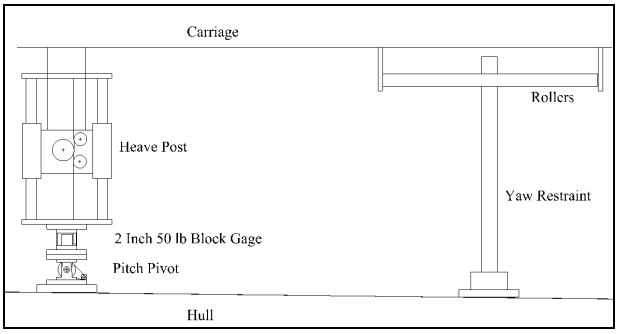

Figure 4 – Sketch of theTowing Rig

The raw data for the four displacements, which were run back-to-back, is presented in Table 1 and is below.

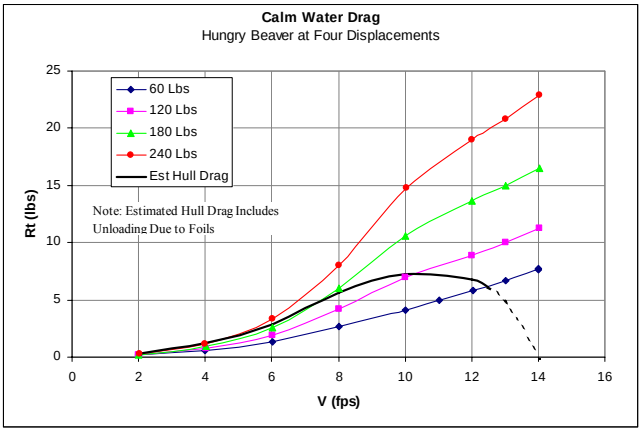

Figure 5 – Calm Water Resistance Data

As speed increases, the foils unload the hull, effectively reducing its displacement. Consequently, it is likely that the contribution of the hull to the total boat drag never exceeds 8 lbs. If the resistance data is normalized by displacement and speed squared, the data for the three highest displacements collapse into essentially one curve. See Figure 6. The relatively greater resistance of the 60 lb displacement is due to its proportionally higher wetted surface. At the light displacement, over half the wetted area is retained, despite shedding ¾ of the weight.

Table 1 – Calm Water Resistance Data

Configuration	V (fps)	Rt (lbs)	Pitch (deg)	Heave (in)
Disp 60lbs Draft 2.2in WS 9.34 sqft	1.988	0.160	-0.012	-0.021
	14.018	7.698	1.188	-0.172
	4.003	0.598	0.030	-0.024
	13.034	6.649	1.100	-0.145
	6.015	1.318	0.015	-0.116
	12.029	5.814	1.023	-0.208
	8.012	2.690	0.423	-0.244
	10.024	4.119	0.836	-0.243
	11.019	4.920	0.910	-0.231
	14.018	7.591	1.168	-0.172
Disp 120lbs Draft 3.6in WS 12.06 sqft	2.011	0.149	-0.029	0.002
	14.037	11.248	1.605	-0.306
	4.008	0.768	-0.028	-0.068
	13.028	10.012	1.509	-0.340
	6.007	1.906	-0.004	-0.175
	12.022	8.862	1.408	-0.353
	8.015	4.244	0.526	-0.398
	10.021	6.931	1.164	-0.419
Disp 180lbs Draft 4.9in WS 14.49 sqft	2.010	0.217	-0.020	-0.036
	14.041	16.538	1.910	-0.470
	4.015	0.946	-0.040	-0.094
	13.033	14.995	1.836	-0.476
	6.012	2.583	-0.017	-0.251
	12.022	13.598	1.723	-0.531
	8.015	6.045	0.538	-0.537
	10.021	10.603	1.454	-0.610
Disp 240lbs Draft 6.2in WS 16.85 sqft	2.013	0.311	-0.022	-0.033
	14.034	22.860	2.078	-0.626
	4.006	1.171	-0.011	-0.138
	13.027	20.763	2.031	-0.664
	6.011	3.294	-0.022	-0.302
	12.023	18.979	1.965	-0.686
	8.022	7.998	0.618	-0.662
	10.029	14.810	1.642	-0.756

Note: Tests were conducted in 65.1°F fresh water

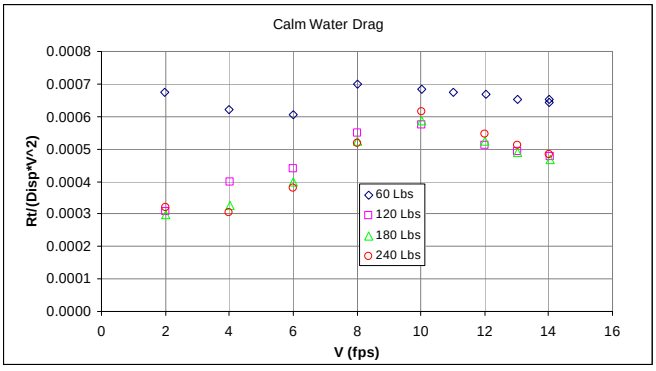

Figure 6 – Collapsed Resistance Data

Figure 7 shows the collected pitch and heave data, although their significance is open to debate. Certainly in light air the boats are sailed with substantial trim down by the bow. Despite greater wetted surface, the reduced transom immersion when sailing bow down almost certainly results in reduced resistance. This effect was not investigated as the constraint of having adequate angle of attack on the foils limits the usefulness of dramatic trim changes.

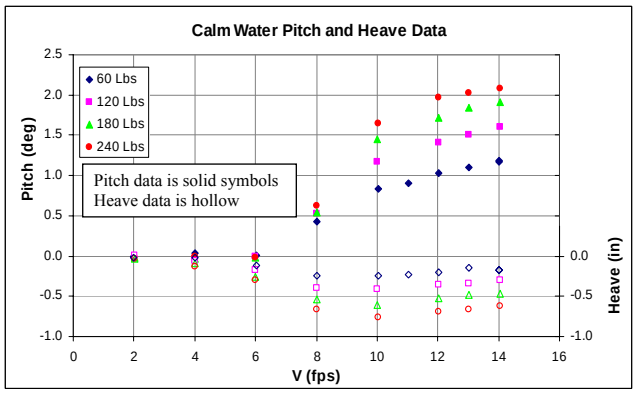

Figure 7 – Pitch and Heave Data

Photographs of the bow and stern waves generated at 13 fps (240 lbs displacement), shown in Figure 8, are typical of the flow observed on the hull.

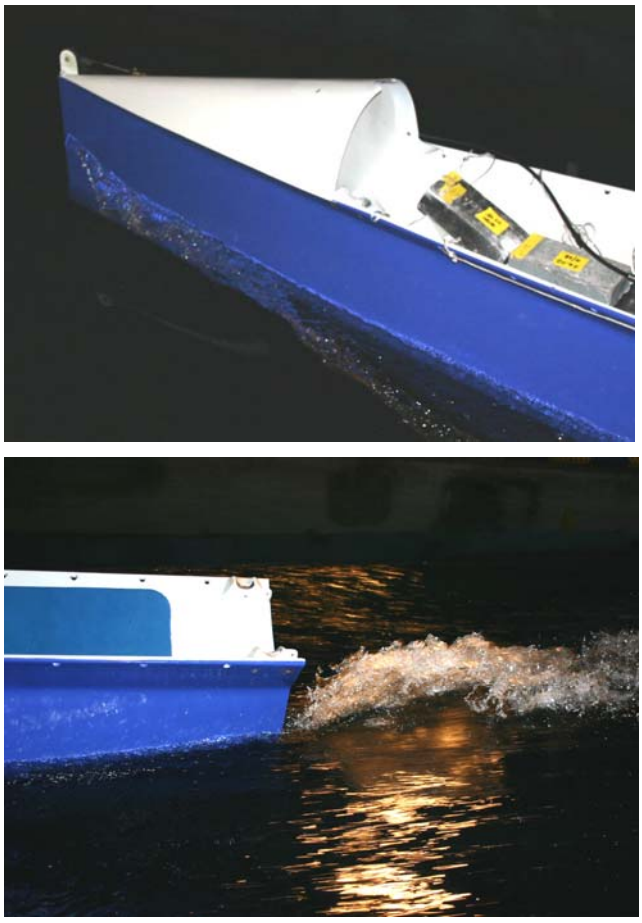

Figure 8 –Hungry Beaver at 13fps Design Displacement

HYDROFOIL EFFICIENCY

Anyone who has designed or built a Moth ruminates about the next generation of foils. What should they look like, what aspect ratio, planform, section? What taper, sweep, washout? What is the penalty for actuating flaps instead of changing the angle of the entire foil? The variables are limitless. Lift and drag characteristics of foil sections are well documented and we are blessed with open airfoil databases and software tools like MIT's *XFOIL* (Drela, 1989) to study design tradeoffs for airfoil sections. But the other features of hydrofoil design are not so well documented. Little nuggets of information from *Fluid-Dynamic Lift* (Horner, 1975) and *Fluid-Dynamic Drag* (Horner, 1965) are about all we have to estimate performance and make tradeoffs on design features like planform, sweep, depth, strut spray drag, junction drag, etc. And these bits of information were usually obtained for much larger and faster vehicles so the Reynolds Numbers are often 2, 3, or even 10 times greater than for Moth foils.

Given the near-infinite list of variables in the design of Moth hydrofoil/strut combinations, our first step was to isolate the measurements that are relatively easy to accomplish and at the same time provide the most useful data. Ideally we would like to obtain lift and drag measurements for the T foil over a range of pitch, leeway, heel, and flap angles. There are two obstacles to that approach: 1) the complexity of measuring six-degree forces and moments, 2) the matrix of test conditions increases exponentially with the number of experimental variables. Given a limited amount of time available in the tank, we felt our time was best spent by limiting the test configurations to a zero roll and zero yaw conditions with only variations in foil pitch and flap angle. It is hoped that this data would be useful in determining the maximum achievable lift to drag ratio of a foil, and determining the effect of depth, junction drag, and various flap geometries.

In keeping with the "Easy to Accomplish" guideline, in addition to the Hungry Beaver foils we were able to borrow for testing the foil sets for two commercially available moths. These components are labeled "Vendor 1" and "Vendor 2" in the following figures. Between them, these two manufacturers share approximately 70% of the market, and gave us the opportunity to compare our foils against the current state of the art.

Instrumentation

The instrumentation used for the foil testing is shown in Figure 9 and 10. It consists of a 250 lb capacity 4 inch block gage measuring lift, and a 50 lb 4 inch block gage measuring drag. The gage calibrations indicate we can resolve lift forces to within 0.4 lbs and 0.1 lbs in drag with a 95 % confidence level (2 standard deviations).

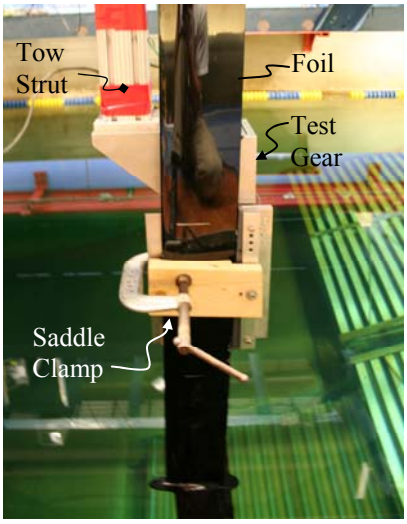

Figure 9 – Overview of T-foil Test Gear

The gages were configured in a simple stack and were affixed to always remain in the carriage axis. Below the gage stack a pitch plate was mounted to allow the angle of the foil to be adjusted in one degree increments over a range of 13 degrees. The foils were clamped in saddles to the pitch plate, insuring that they remained at zero yaw. Figure 10 shows a photograph of the backside of the gage stack showing the force gages and the frontside of the gage stack showing the pitch plate.

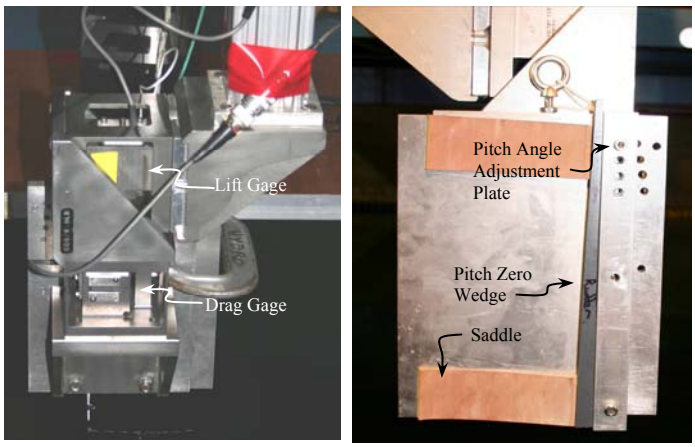

Figure 10 – Details of T-foil Test Gear

The depth of the foil in the water was adjusted by sliding it up and down in the saddles and clamping it at the appropriate height. Foil immersion was measured vertically from the water surface to the nominal centerline of the lifting foil at the ¼ chord.

Test Plan

The lift and drag of the struts and foils were characterized for several simplified operating conditions.

1) Drag of the vertical struts was measured at zero angle of attack and two submersion depths (12 and 24 inches) for speeds ranging from 10 to 30 fps. These tests allow the total strut drag to be partitioned into a section drag component and a wave and spray drag component.

2) Lift and drag of the T foil were measured when operating upright (zero roll), at zero yaw, 20 fps, and various pitch angles and no flap angle. Most tests were run at 18 inches immersion; however several depths were tested to asses the tradeoff between vertical strut drag and hydrofoil wave drag.

3) Lift and drag of the T foil were again measured at zero roll, zero yaw, 20 fps, and 18 inches immersion, but the flap angle was varied for a given pitch angle to achieve a constant lift of 180 lbs. This highlights the effect of the flap on the system efficiency and provides some guidance how best to set up the boat.

20 fps (11.8 knots) was selected for the bulk of the testing because it is a plausible upwind foiling speed, and can be reasonably achieved in the Naval Academy's 380 ft tow tank. The daggerboard loading of 180 lbs was somewhat arbitrarily determined based on a 240 lb sailing weight assuming ¾ of the load on the daggerboard. Likewise, the 18 inch foil immersion was selected as typical from photographs of foil borne Moths. While these simplified test conditions are obviously not fully representative of the conditions that the foils see while sailing (i.e. when they are subject to yaw and roll), the simplification does keep the test matrix manageable and provides a first step in experimental validation of foil performance.

Geometry

The geometries of the tested foils are shown in Figures 11-13. The wing profiles were obtained by digitizing a tracing of the foil planform. The section shapes were obtained by potting templates onto the foil using polyester body putty (Bondo). These templates were then cleaned-up, scanned, and used as input to a drawing program (Rhino). The designed section shapes, where known, are listed with the geometry.

When testing the struts alone, faired end caps were added to the foils to standardize the geometry and minimize end effects. The endcaps were square in planform and section and provided a "prismatic" end to the foils. They were created by the judicious application of bondo shaped with thin Mylar sheet and Formica clamped to the foil. A typical endcap is shown in Figure 14. End caps were applied to all struts except the Vendor2 rudder foil which had a permanently attached lifting foil and tiller fitting, which effectively precluded strut only testing.

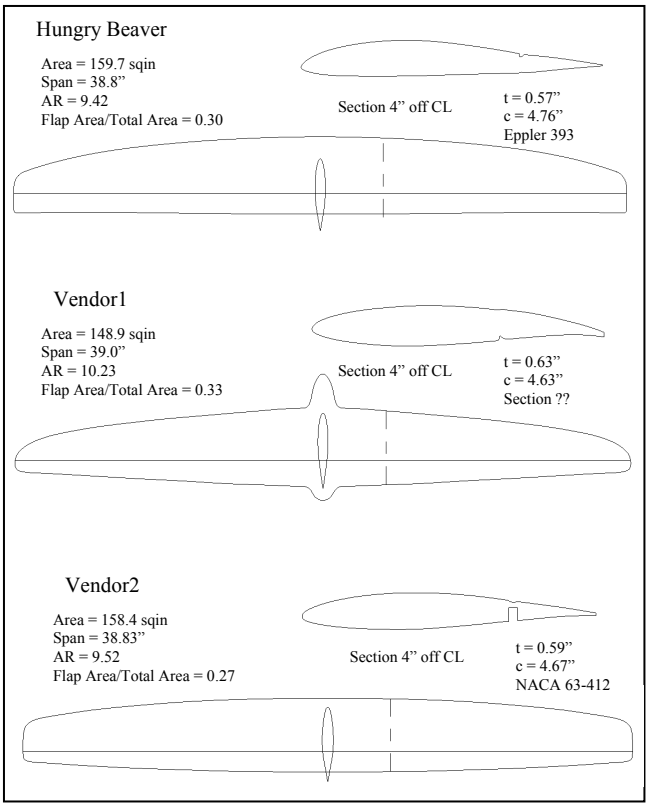

Figure 11 – Geometry of Tested Daggerboard T-Foils

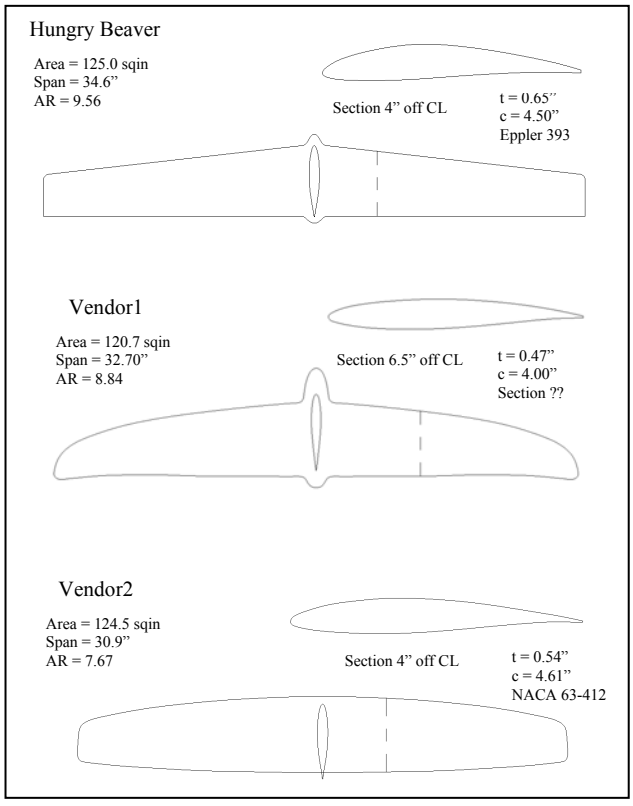

Figure 12 – Geometry of Tested Rudder T-Foils

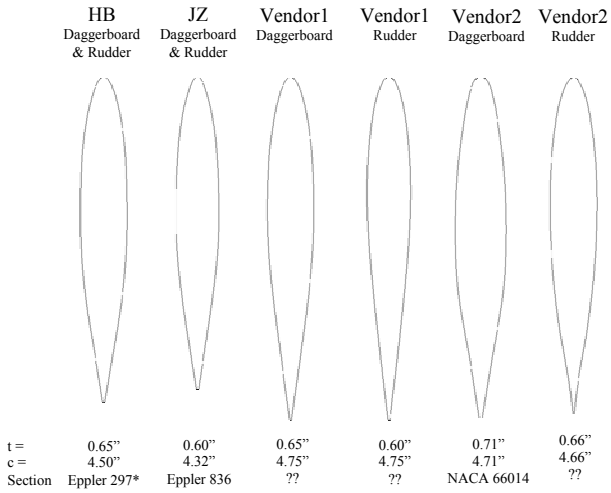

Figure 13 – Geometry of Tested Struts

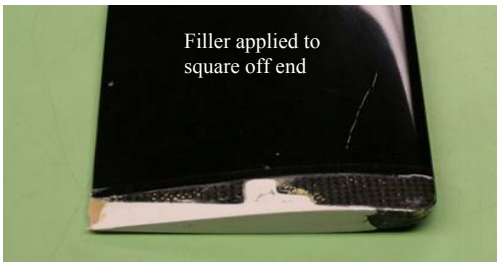

Figure 14 – Prismatic Strut Ends

Flap angle on the daggerboards was adjusted using the existing linkages in the foil. To achieve an accurate and repeatable angle measurement an extended pointer was added to the existing flap linkage which read on a calibrated scale. The linkage was in turn locked in place by nuts on a threaded rod. The entire assembly was judged to be accurate within 0.25 degrees. A typical flap adjustment rig is shown in Figure 15.

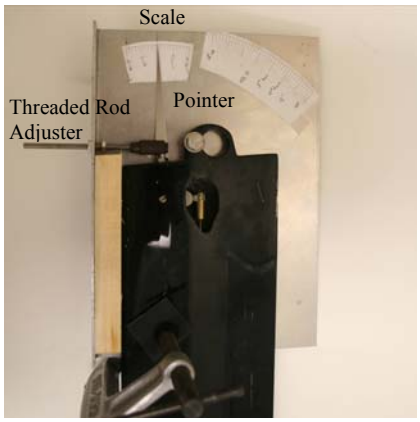

Figure 15 – Flap Adjustment Mechanism

Despite being similar in size, the details of the foil joints varied considerably between the six T Foils. The HB lifting foils employed an approximately 0.75" radius fillet at the T joints. The lifting foil on the HB daggerboard was set forward of the leading edge of the strut, while the leading edges of the lifting foil and the strut were aligned on the rudder T-foil. The Vendor1 lifting foils incorporated a body of revolution at the T junction to facilitate the removal of the foils for storage and transport. The Vendor2 lifting foils have essentially no fillet at the joint and the leading edges of the lifting foils were ahead of the leading edge of the struts. All the T-foils were tested with a spray painted finish, with the exception of the initial tests of the HB dagger board. This test was conducted with "mold finished" surface, however anomalous results lead to the filling, fairing and painting of the HB foils for latter testing.

Results

The performance of a T-Foil can be gauged by the magnitude of the drag penalty while generating the required lift. Figure 16 compares the six T-foils tests on this basis (all at V=20fps, 18 inches immersion, 180 lbs lift for daggerboards, 60 lbs lift for rudders). The drag reported for the daggerboard T-foils is at their most efficient pitch and flap angle to achieve 180 lbs lift.

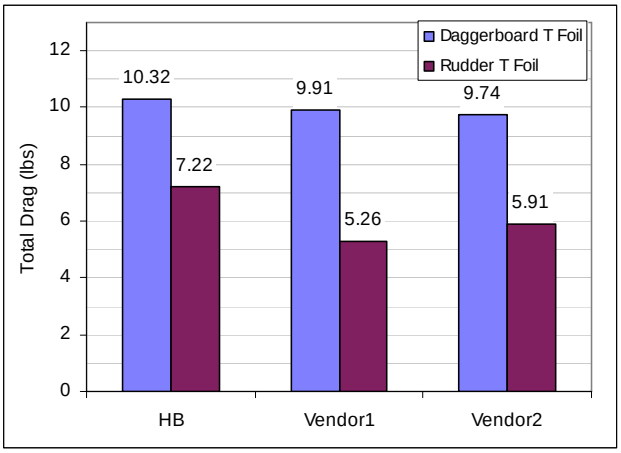

Figure 16 – Drag of T-foils at Operating Condition

The performance of the daggerboard T-foils is fairly similar. The HB rudder foil, however, is clearly inferior. While knowing the total drag of the T-foils while producing the specified lift (180 or 60 lbs) allows them to be ranked, the lift to drag ratio does little to explain what aspects of a particular foil are responsible for the performance. T-foil drag can be divided into the following components:

- Strut Section Drag
- Strut Wave and Spray Drag
- Junction Drag between the Lifting Foil and Strut
- Lifting Foil Section Drag
- Lifting Foil Induced Drag
- Lifting Foil Wave Drag

Analysis of the data sets allows some of these components to be quantified. For those wishing to perform their own analysis, all the raw data collected on the foils is included in an appendix to this paper.

Strut Data:

Evaluation of the strut drag was relatively straight forward as the struts were run without the lifting foils attached at speed from 5 to 30 fps. The raw strut data was first converted to a total drag coefficient and faired across speed for each depth to get a faired resistance. The parasitic drag due to the prismatic foil end was estimated based on the Hoerner formulation:

$$\text{Drag} = \tfrac{1}{2}*0.15*(0.5*\rho*V^2*t^2)$$

and subtracted from all the data. The wave and spray drag was then calculated as:

$$Rt_{Wave\&Spray} = 2 * Rt_{faired\ 12"immersion} - Rt_{faired\ 24"immersion}$$

The wave and spray drag was converted into a coefficient according to the Hoerner formulation where t is the foil thickness:

$$Cd_{W\&S} = Rt_{Wave\&Spray}/(0.5 * \rho * V^2*t^2)$$

For the five speed run, the highest and lowest values for the coefficient were disregarded and the middle three were averaged to determine the reported wave and spray drag coefficient shown in Figure 17. A typical photograph of the spray generated is shown in Figure 18.

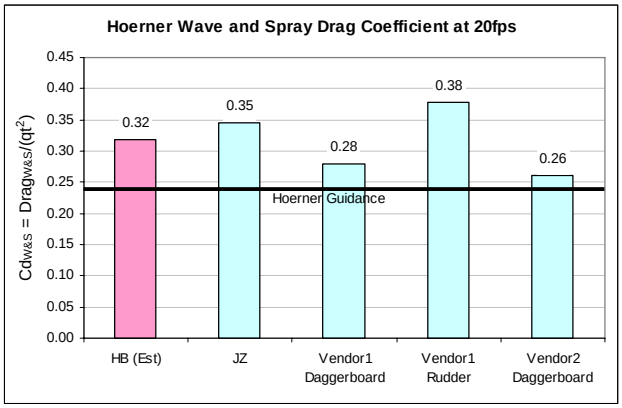

Figure 17 – Calculated Wave and Spray Drag Coefficient for Struts

Figure 18 – Spray Generation off the Vendor2 Daggerboard T-Foil at 20 fps

The section drag coefficient for each speed and depth was calculated as:

$$Cd_s = (Rt_{faired} - Rt_{Wave\&Spray})/(0.5 * \rho * V^2*S)$$

These drag coefficients were then averaged across both speed and depth to get the final section drag coefficient for a particular strut section, shown in Figure 19. It should be noted that anomalous data on the HB strut resulted in the use of the averaged wave and spray drag data from all the struts for the HB strut calculations.

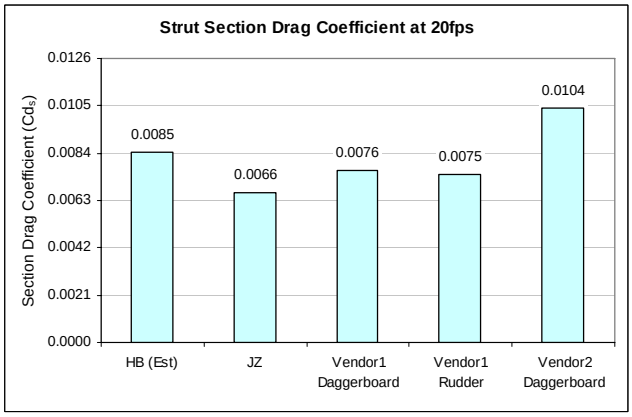

Figure 19 – Calculated Section Drag Coefficient for Struts

The strut analysis brings home several points:

- The wave and spray drag of the struts is some 30% higher than would be anticipated based on simple calculation from Hoerner.
- The Reynolds number effects are significant on the strut performance. Guidance from (Abbott and VonDoenhoff, 1959) would suggest minimum section drag coefficient of 0.005-0.006 is acheivable. The lowest Reynolds number data in (Abbott, 1959) is $3*10^6$ whereas the struts operating at 20 fps are at $Rn=6*10^5$. (Lyon, 1997) suggests a section drag coefficient nearer 0.008 is appropriate at $Rn=5*10^5$, which conforms well to our data. It is interesting to note however, that the most aggressive laminar section, the Vendor2 daggerboard strut, does not appear to be benefiting from a drag bucket.
- Thinner is better. Certainly, in straight ahead tests thinner foils performed better, the limit being structural. It is unknowen if this trend would hold if yaw were considered.

With the section and wave and spray drag coefficients, the foil drag for the 18 inch strut immersion could be calculated. If this is then subtracted from the T-foil drag, the result is the total lifting foil drag, including junction drag, section drag, induced drag, and wave drag.

Lifting Foil Wave Drag:

The lifting foil wave drag can be isolated by looking at the variation of foil drag against depth at nominally constant lift. By plotting against the chord to depth ratio of the lifting foil (c/h), the drag of the lifting foil at infinite depth (c/h = 0, no wave drag) can be established. This is shown in Figure 20 for all the foils except the Vendor1 daggerboard, for which no varying depth data was collected.

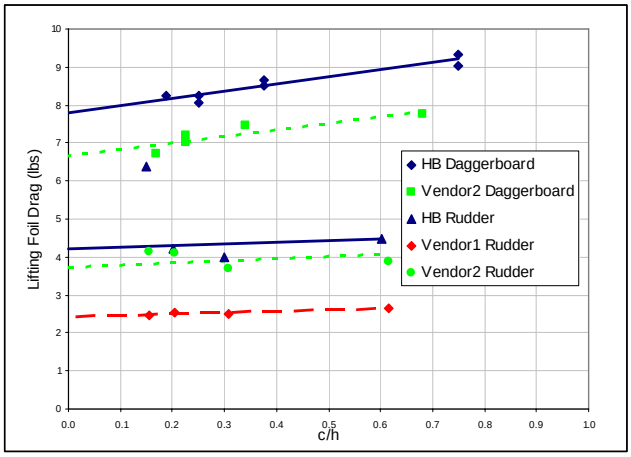

Figure 20 – Lifting Foil Drag extrapolation to Infinite Depth

Knowing the lifting foil drag without wave making, it is a simple matter to back-calculate the drag associated with wave making for each lifting foil. This can then be converted into the Hoerner formulation of wave drag and solved for $C_{DH}/C_L^2{}_H$:

$$Cd_{Wave} = Rt_{Wave}/(0.5* \rho*V^2*S) = C_L^2 * c/h * C_{DH}/C_L^2{}_H$$

The resultant values of $C_{DH}/C_L^2{}_H$ are:

HB Daggerboard	0.026
Vendor2 Daggerboard	0.024
HB Rudder	0.022
Vendor1 Rudder	0.039
Vendor2 Rudder	0.022

The lifting foil wave drag coefficient is gratifyingly consistent, but is on the order of half the value predicted by Hoerner. Certainly the lightly loaded rudders show little wave drag penalty for operating near the surface, but the maneuvering implications for operating very near the surface are grave indeed. The more heavily loaded daggerboards gain about a pound of wave drag operating near the surface, but this is offset by the reduction in strut drag. This result confirms what Moth sailors have discovered; the higher you fly, the faster you go.

Induced Drag:

Without knowing how section drag varies with lift coefficient it is not possible to extract the actual induced drag from the data. Consequently the simple formulation of $Cd_{induced} = C_L^2/(2\pi*AR)$ was used to ballpark the induced drag (drag due to lift) on the foils. The induced drag is about a quarter of the daggerboard T-foil drag, but only about 5% on the lightly loaded rudder. This outcome can be viewed in two ways: 1) The higher percentage of induced drag on the daggerboard T-foil could be an indication that a higher aspect ratio on the daggerboard lifting foil would be appropriate. Increases in aspect ratio are however, limited by structural implications. 2) The lower proportion of induced drag on the rudder T-foil is probably an indication that the rudder lifting foil is too large, or that the assumed rudder loading is not representative of what the rudder actually encounters.

Section and Junction Drag:

After eliminating the strut drag, the lifting foil wave drag, and the induced drag, we are left with a rather substantial chunk of drag that is attributable to the lifting foil section drag (including the parasitic effects of the flap joints) and the junction drag between the strut and the lifting foil. Unfortunately this cannot be parsed further with the available data. Hoerner suggests that the junction drag can be estimated as:

$$\Delta D=C_{Dt}*(0.5* \rho*V^2*t^2)$$

where $C_{Dt}=17*(t/c)^2-.05$ and t = average thickness

Using this formulation, the junction drag would account for less than 10% of this remaining drag piece. A comparison of the combined section and junction drag converted into a coefficient form based on the lifting wing planform area is shown in Figure 21. The foil loading for this comparison is 180 lbs for the daggerboard ($C_L \sim 0.43$) and 60 lbs for the rudder ($C_L \sim 0.18$)

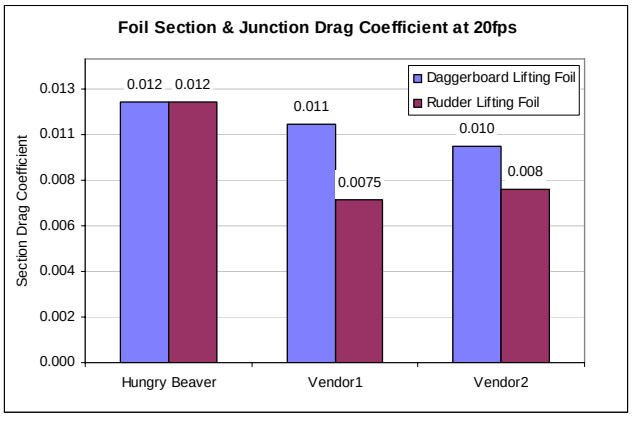

Figure 21 – Section and Junction Drag of Lifting Foils

The high section and junction drag of the HB rudder stands out and is clearly the cause of its poorer performance. The HB rudder foil is both thicker and more highly cambered than the commercial vendor products. It was originally designed as a one size fits all foil design that could be used for both the main lifting foil and the rudder. It has proved not very good at either. Moreover the alignment of strut and foil leading edges likely creates the

highest junction drag of the tested foils.

As observed with the struts, the lifting foils are operating at low Reynold numbers ($6*10^5$) which probably preclude section drags much lower than the 0.007 range observed in the commercial vendor rudders. The higher section and junction drag coefficients observed on the daggerboards verses the commercial rudders is likely due to the slightly greater t/c ratios of the daggerboards and the parasitic drag associated with the flap joint. Both commercial daggerboards had flaps which were mechanically connected to the main portion of the foil by a fabric hinge faired on the upper surface with flexible caulking. This construction method results in a gap on the lower foil surface necessary for foil articulation. Figure 22 shows this flap configuration and an alternative used on the HB daggerboard foil to eliminate this gap. It was hoped that eliminating the gap would result in decreased section drag.

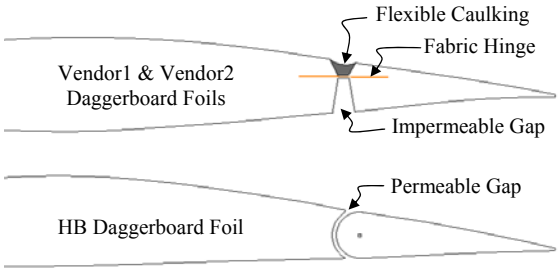

Figure 22 – Construction Details of Flaps

The test results do not show any improvement associated with the HB flap construction method, however the effect may be masked somewhat by an additional structure added to the underside of the foil and flap necessary to stabilize the T joint. The initial test results on the HB daggerboard foil indicate that a permeable hinge joint which allows pressure relief across the foil may well be a greater liability than a larger impermeable hinge gap. In the subsequent painting and fairing of the foil this gap was minimized to the extent practicable.

Summary Drag Breakdown:

Figure 23 summarized the drag breakdown for the six T foils tested. Small gains could probably be realized by pushing material limits harder and making thinner foils. The greatest area for improvement, however, looks to be the size of the rudder lifting foil. Over 50% of the drag of the rudder is associated with the section and junction drag of the lifting foil. Given the relatively small amount of lift the rudder carries, some experimentation with a bandsaw looks appropriate.

All the foil testing discussed thus far assumes a plausible upwind speed of 12 knots. Off the wind, a Moth is capable of better than twice that speed. The total vertical force required of the foils, however, remains constant. Some boats have experimented with pitching the entire daggerboard foil to control vertical lift, but the vast bulk of current moths modulate the lift using a surface sensing

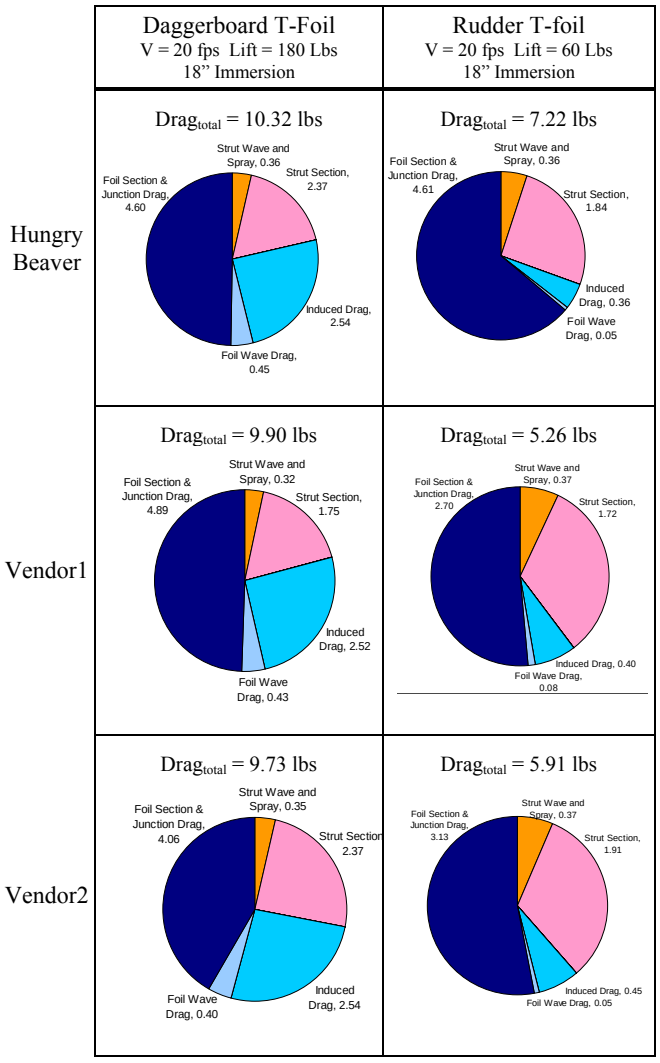

Figure 23 – Summary of T-foil Drag Breakdown

wand at the bow which articulates the main foil flap through a series of linkages. The authority of a ~30% flap at modulating lift is about 45% of what would be achieved by globally changing the angle of attack of the lifting foil. Put another way, a 2.2 degree change in flap angle is required to obtain the same result as a 1 degree foil change. Although not intuitive, from a sailing perspective flap up (shedding lift) is more important than flap down (adding lift) because of the dire nature of the crash that comes from the inability to shed lift adequately. The efficiency of the flap can be gauged by its impact on the L/D ratio in off design conditions shown in Figure 24.

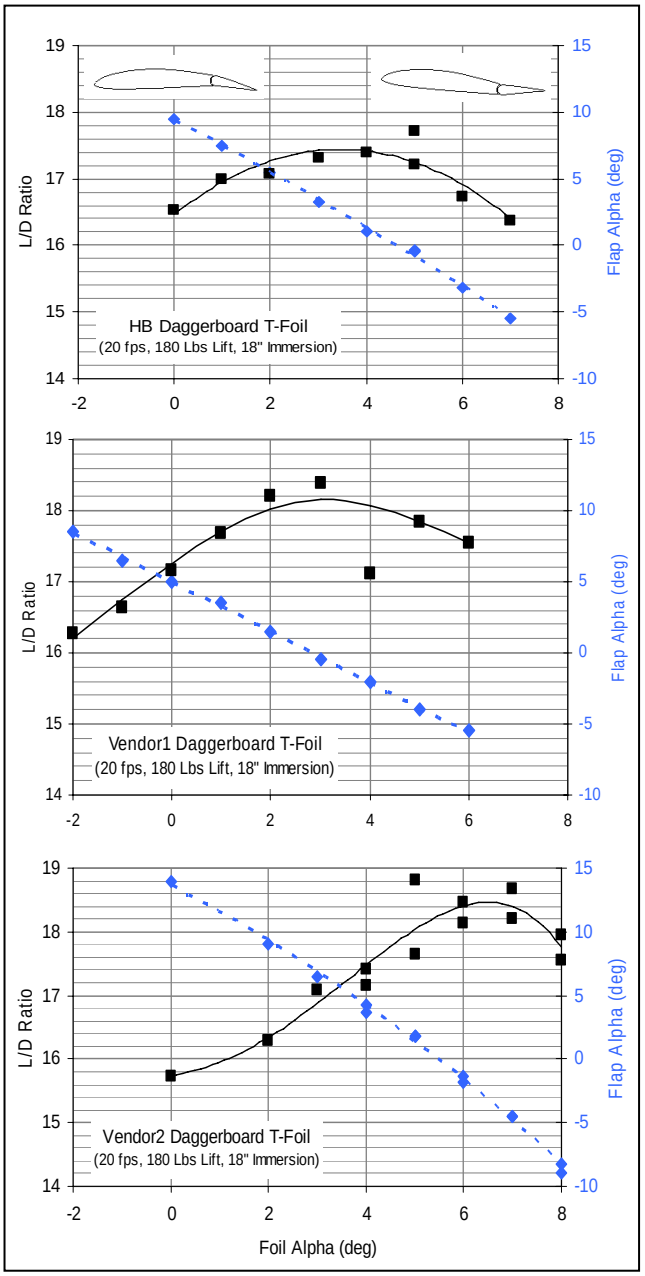

Figure 24 – Impact of Flap angle on L/D ratio

Surface Finish:

(Schultz, 2004) showed the parasitic drag coefficient of a foil in our Rn range to be insensitive to surface finish. Although no similar controlled experiment was conducted, the initial test of the HB daggerboard and strut were conducted with a "mold" finish (It's hard to justify working hard on a foil, that may well not last through your next sail). The mold finish surface, although reasonably fair, had a significant number of pin holes in the weave of the carbon cloth and some deep grooves along the foil leading edges where the two halves were bonded together. Tests showed the drag of the struts and foils tested in this condition to be approximately 25% greater than later tests where the foils were filled, faired and painted. Most sailors obsess about the surface finish of their foils and the antidotal evidence from these tests indicate that they are right in doing so.

AIR RESISTANCE TESTS

When Moths are sailed fast with their hull completely out of the water, aerodynamic drag has to be an important component in the overall drag picture. It is difficult to estimate drag coefficients given the unusual hull and hiking rack configuration so a plan was made to conduct tests of the hull in air, measuring drag and side force directly. It would have been valuable to include a study of drive and side force on the sail and rig but that was well out of reach given the time and resources available. As an afterthought, we decided to include a dummy helmsman on the boat who we named Gui in honor of a local Mothie. It was a good thing that Gui went along for the ride because he was found to contribute considerably to the total aerodynamic drag.

Once again there were endless combinations of test parameters that could be varied for these tests. To get the most useful information from the time available we settled on modeling one typical upwind case, which assumed a port-to-starboard tacking angle of 96 degrees, a leeway angle of 4 degrees and a boat speed equal to true wind speed of 12 knots. Unlike most other sailing dinghies, Moths sail upwind most efficiently when heeled well to windward.

Figure 25 – Force Diagram when heeling to windward

Windward heel, shown in Figure 25 has multiple benefits:

- it increases the righting arm between the foil lifting force and the hull and helm weight
- it produces a side force component from the lifting foils that augments the side force generated by the struts to reduce leeway. This is critical if strut area (and drag as we have seen) is minimized by flying high
- it produces a lift component from the sail force that reduces the lifting foil loading
- it shifts the helmsman closer to the water decreasing the impact of his wind shadow on the sail and putting him in a slower moving portion of the wind boundary layer

Off the wind, windward heel has little effect on performance and the boats are typically sailed upright. Given the various sailing attitudes and the wide hiking racks, it seemed prudent to test at multiple angles of heel.

Test Setup

The original plan was to tie the boat on top of a car with an instrumented platform between the car and boat. This would have provided great entertainment for our co-workers, but the plan was eventually scrapped in favor of using the towing carriage in our more controlled laboratory environment. A platform was built and mounted on sliders supported by rails. The boat was tied to the platform and the force parallel to the rails was measured using a single force gage. Drag or side force could be measured separately using the same rails and force gage but with the hull at different orientations on the platform. After several days spent in the tank trying to get the rail-and-slider rig to produce reliable measurements, the rig was finally abandoned. This exercise lead to the development of a new rig in which the boat was mounted directly on top of a stack of two force gages. Both the boat and original platform were mounted on top of the gages with wedges inserted to heel the boat to angles of 0, 15 and 30 degrees. Figure 26 shows the final air resistance test setup without the helmsman while Figure 30 shows the test set-up with the dummy helmsman.

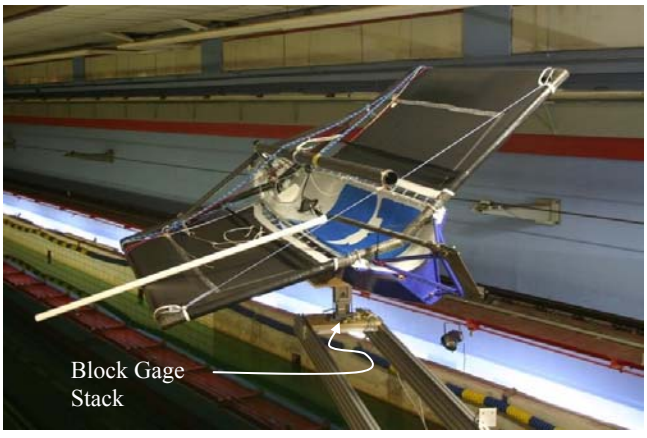

Figure 26 – Aerodynamic force measurement rig mounted on frame in front of towing carriage

The force gages used for these tests were four inch cubes similar to those used for the other tests reported in this paper. The gages had a capacity of 100 lbs and were calibrated immediately before the tests. The expected accuracy is +/- 0.01 lbs, based on two times the standard deviation of a 10 point calibration.

To allay concerns about interference to the airflow in the vicinity of the carriage an aluminum frame was used to move the center of the model out approximately eight feet forward of the carriage. Airspeed around the hull was measured with the carriage underway using a Davis 271 Turbo Meter anemometer. The anemometer was attached to the end of a long stick and wind speed was surveyed at several locations around the hull. For all locations the wind reading matched the carriage velocity within 0.5 ft/sec, which was about equal to the accuracy of the anemometer, so no further corrections were made and wind speed was assumed to be equal to carriage speed.

Force Measurement Conventions

Figure 27 shows a conventional breakdown of aerodynamic and hydrodynamic force components. The aerodynamic force component of interest is the force parallel and opposite to the direction of the boat's motion i.e. that which slows down the boat. This force component will be hereafter referred to as aerodynamic drag and should not be confused with the component parallel to the apparent wind velocity.

Figure 28 shows a wind diagram in what was considered to be a typical upwind Moth sailing condition: beating upwind with a true wind speed of 12 knots and a boat speed of 12 knots. It may be surprising to note that the apparent wind speed for this condition is 21.9 knots. Again, the drag of interest is the force component in the direction of boat motion so the force gages were aligned at 0 and 90 degrees relative to the course made good (see Figure 29).

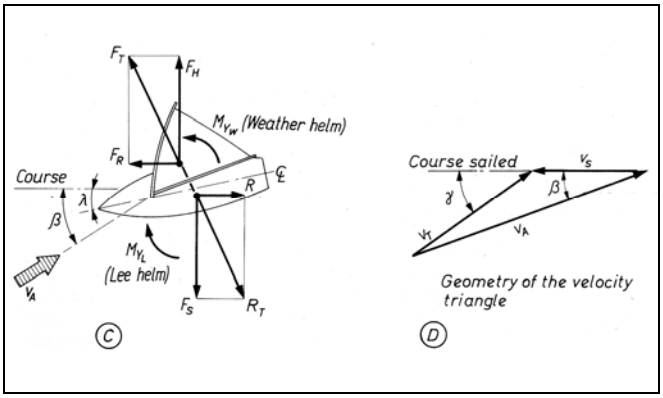

Figure 27 – Conventional aerodynamic and hydrodynamic force components (Marchaj, 1990)

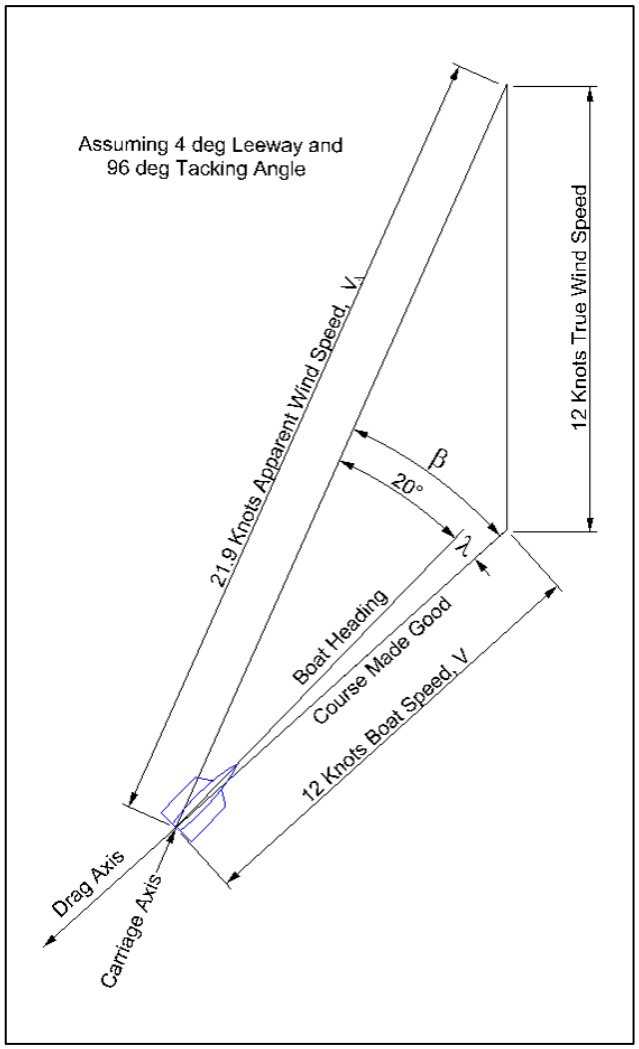

Figure 28 – Apparent wind when beating assuming a 96 degree port-to-starboard tacking angle

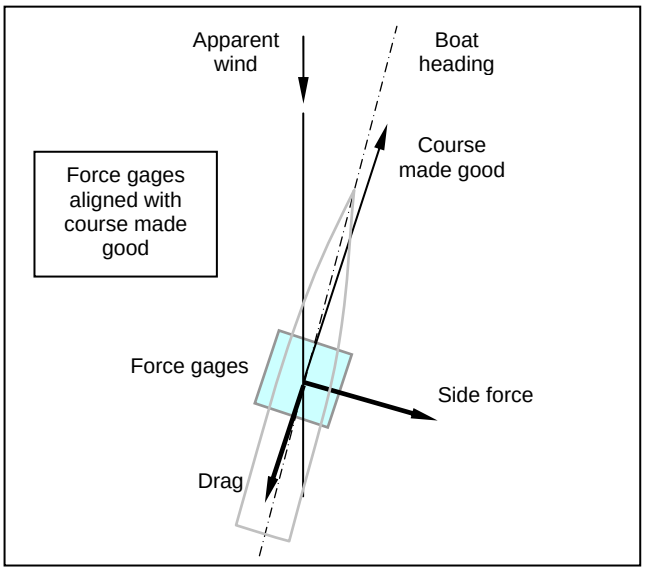

Figure 29 – Aerodynamic force gage axes

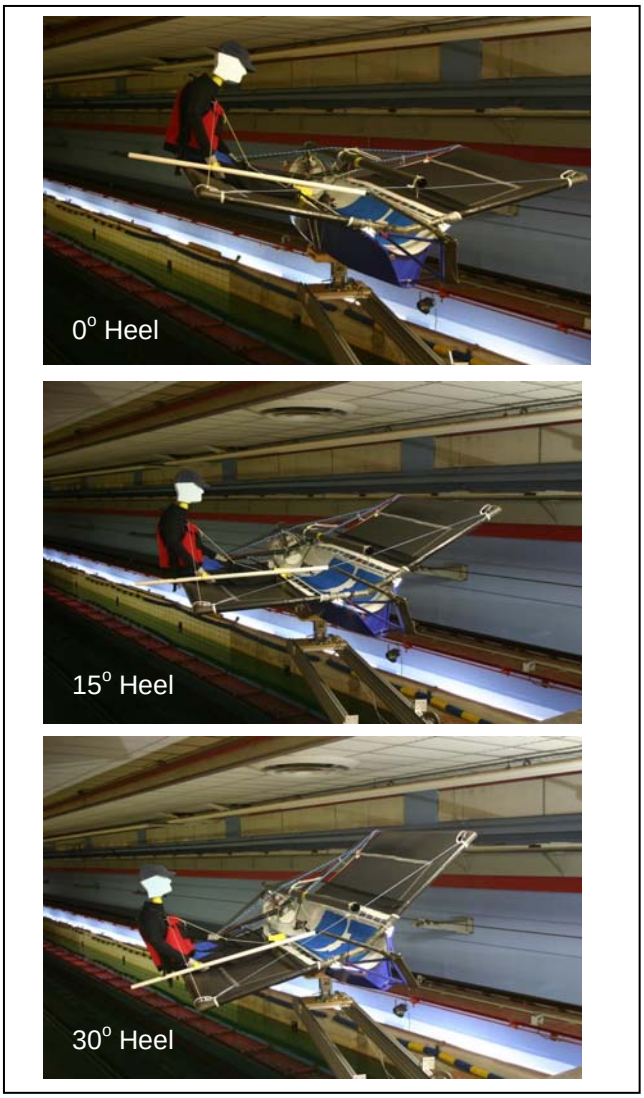

Figure 30 – Boat with dummy helmsman

Test Results

The original plan was to run a matrix of tests varying wind speed, heel angle and crew (with or without helmsman). Since half of the available test time was spent de-bugging the first unsuccessful test rig, the speed variation was eliminated from the test matrix to save time. A carriage speed of 20 fps was chosen for all of the tests to keep the forces to a reasonable level. If it is assumed that the drag coefficient is relatively constant with changes in speed, the drag at other speeds can be estimated using the factor R/V^2.

Five repeat tests were run for each condition to home in on mean force values. The scatter in the data was assumed to be caused by large scale turbulence and separation off of the hull, appendages and helmsman. With average drag values of around 3 lbs and five repeat tests there was a typical standard deviation of 0.1 lbs (3% of 3 lbs).

Table 2 shows a summary of the mean air resistance forces in pounds normalized by velocity squared. The normalized values are plotted in Figures 31 and 32. It is interesting to see that the highest aerodynamic drag was measured with the hull upright. This was not anticipated but by looking at the boat from the "winds eye view" in Figure 33, it appears that the dihedral of the windward hiking rack may be the source of the higher drag. Side force vs. heel angle is plotted in Figure 32 which shows that side force is relatively constant with varying heel angle.

An important observation from Table 2 is that the helmsman makes up 42 percent of the total aerodynamic drag and only 4% of the aerodynamic side force.

Table 2 – Summary of average measurement values for Apparent Wind Speed = 20.05 fps (11.88 kts)

Helms-man	Heel (deg)	Drag (lb)	Side F (lb)	Drag/V^2 (lb/fps^2)	Lift/V^2 (lb/fps^2)
with	0.0	3.84	4.94	0.0095	0.0123
with	15.0	3.13	4.61	0.0078	0.0115
with	30.0	2.99	5.51	0.0074	0.0137
w/o	30.0	1.73	5.28	0.0043	0.0131

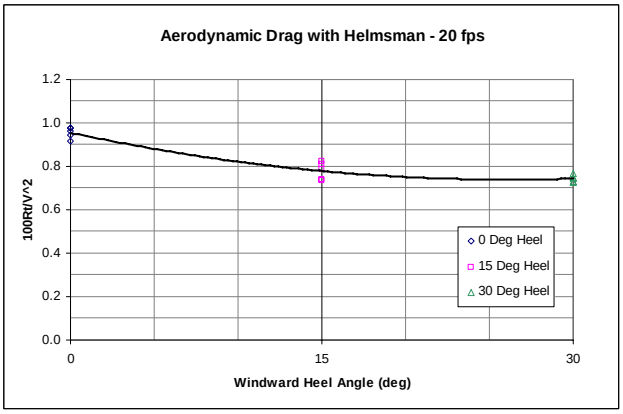

Figure 31 – Aerodynamic drag normalized by V^2

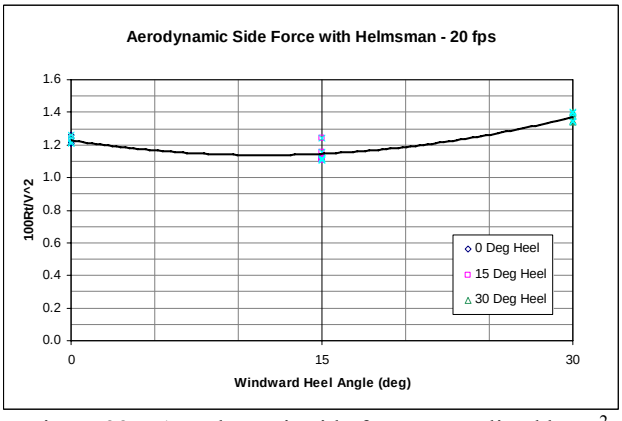

Figure 32 – Aerodynamic side force normalized by V^2

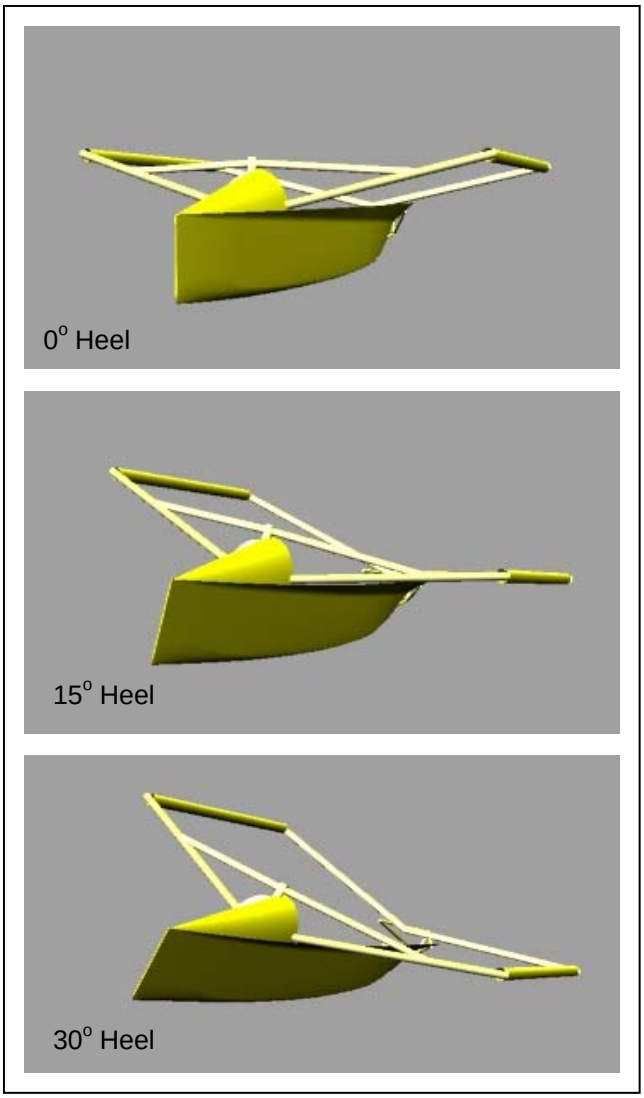

Figure 33 – "Wind eye view" of boat when heeled

The forces listed in Table 2 represent an apparent wind speed of 20 fps. The upwind condition in Figure 28 shows an apparent wind of 21.9 knots or 37 fps. For a ballpark idea of drag and side force over a range of speeds, Table 3 was prepared assuming constant values of [drag/V^2] = 0.80 and [side force/V^2] = 1.2. In order to calculate apparent wind speed it is necessary to estimate the boat speed for a given wind speed and assume tacking and leeway angles. For the table it was assumed that when beating to windward, the boat speed was equal to the true wind speed, the tacking angle was 96 degrees and leeway 4 degrees. These are broad assumptions but show the order of magnitude of the aerodynamic drag forces. The tabulated drag numbers are plotted in Figure 34.

Table 3 – Estimated aerodynamic force vs. boat speed when beating upwind

Boat Speed (kts)	True Wind Speed (kts)	Apparent Wind Speed (kts)	Apparent Wind Speed (fps)	Aero Drag (lb)	Aero Side F (lb)
0	0	0.0	0.0	0.0	0.0
10	10	18.3	30.8	7.6	11.4
12	12	21.9	37.0	11.0	16.4
15	15	27.4	46.3	17.1	25.7
20	20	36.5	61.7	30.4	45.7

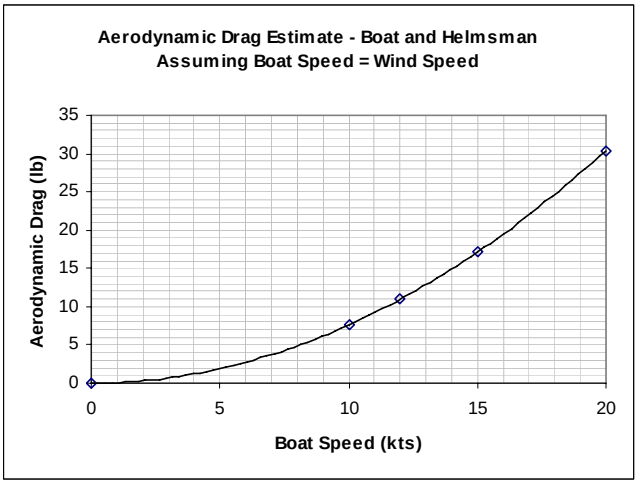

Figure 34 – Aerodynamic drag vs. speed

Currently, hydrofoil Moth speeds have been clocked in the 28 knot range but that is only off the wind. When beating upwind, typical sailors hit speeds of 10-14 knots and top sailors reach 15 knots. At 15 knots, Table 3 shows an aerodynamic drag of 17 lbs. This is about 70% of the total hydrofoil drag, so it appears that the aerodynamics of the boat are now nearly as important as the hydrodynamics.

SUMMARY AND CONCLUSIONS

After nearly 100 hours of work and 340 carriage runs equating to nearly 20 miles of data collection, we have made a start at exploring the hydrodynamic and aerodynamic characteristics impacting Moth design. The complexities of optimization of a hydrofoil sailboat are not simple and many questions remain unanswered. It is hoped that the data presented in this paper will provide a solid technical basis for further performance improvements by motivated designers and builders. The primary factors governing performance of a hydrofoil moth hull have been documented. Several foil systems have been studied and the results parsed to identify areas improvement. Some of the primary conclusions derived from this work are:

- Aerodynamic drag plays nearly as great a role in upwind speed as hydrodynamic drag. Reductions in aerodynamic drag through smaller hulls, cut away tramps, faired tubing , etc. could well be meaningful.
- It is possible for a motivated amateur to build a boat on par with the commercial offerings (or nearly so). Further incremental improvement in the hydrofoil efficiency appears possible by exploiting advanced materials to achieve thinner struts and foils.
- Higher is better. The hydrodynamic drag on the foils decreases with reduced immersion. Increased foil wave drag is not significant. The feedback control systems to hold altitude have improved markedly in the last year or two, allowing sailors to fly higher with less risk of crashing. Further efforts spent to reduce foil immersion will improve performance.
- Existing rudder lifting foils appear too large. Experiments with smaller foils may yet lead to improved performance.

By their very nature development classes evolve over time. The amazing performance of the current hydrofoil Moths can be traced from their origins in the conventional dinghy designs of the 1930s to the scows of the ‘60s, to the progressively narrower skiffs of the ‘80s and ‘90s, to a plethora of hydrofoil concepts, to the current bi-foiler design. Development will continue, and it will be fun to see what the boats will look like a decade or two hence.

ACKNOWLEDGEMENTS

The authors would like to express their appreciation to Professor Greg White, the Naval Academy Hydromechanics Lab Director, for allowing us to use the lab facilities and supporting these tests. Additionally, we would like to thank Karl Wittnebel, Joe Cummings, and Nik Vale for making the vendor foils available for testing. Lastly, we’d like to acknowledge Guillaume Vernieres, whose skill as a builder and sailor and enthusiasm for the hydrofoil moths is in no small way responsible for our involvement in this diverting activity.

REFERENCES

Abbott, Ira H. and VonDoenhoeff, Albert E., "Theory of Wing Sections" Dover Publications Inc., 1959.

Drela, M., XFOIL: An Analysis and Design System for Low Reynolds Number Airfoils, Conference on Low Reynolds Number Airfoil Aerodynamics,
University of Notre Dame, June 1989.

Hoerner, S. F., "Fluid-Dynamic Drag" Published by author, 1965.

Hoerner, S. F., "Fluid-Dynamic Lift" Published by author, 1975.

Lyon, Christopher A., et al., "Summary of Low-Speed Airfoil Data Volume 3", SoarTech Publications, 1997.

Marchaj, C., "Aero-Hydrodynamics of Sailing", International Marine Publishing, 1990.

Schultz, M., Esquivel, C., and Miklosovic, D. "Effect of Surface Finish on Aerodynamic Performance of a Sailboat Centerboard", Journal of Aircraft 2004.

Appendix A – Raw Data

Geometry	Data File	Velo (fps)	Lift (lb)	Drag (lb)	Foil Pitch Angle (deg)	Flap Angle (deg)	Depth (in)
Hungry Beaver	123	20.04		1.74			12
Vertical	124	10.02		0.53			12
Strut	124	15.03		1.03			12
	125	20.04		1.66			12
	126	25.05		2.53			12
	127	30.05		3.51			12
Fresh Water	128	20.04		1.65			12
T = 63.0 F	129	10.02		1.04			24
	129	15.04		1.91			24
	130	20.04		3.27			24
	131	25.05		4.73			24
	132	30.05		6.74			24
Hungry Beaver	133	20.05	169.08	9.35	2.08		18
Rudder	134	20.04	133.52	8.35	1.08		18
T Foil	135	20.04	108.46	7.63	0.08		18
	136	20.05	79.56	7.26	-0.92		18
	137	20.05	53.56	7.04	-1.92		18
Fresh Water	138	20.05	39.32	7.12	-2.50		18
T =63.0 F	139	20.05	3.28	7.46	-3.50		18
	140	20.05	-16.01	8.15	-4.50		18
	141	20.05	-38.66	9.32	-5.50		18
	142	20.05	54.49	8.36	-1.50		24
	143	20.05	67.42	7.23	-1.50		18
	144	20.05	67.24	6.26	-1.50		12
	145	20.05	63.17	5.76	-1.50		6
Hungry Beaver	158	20.05	6.44	6.93	0.0	0.0	18
Daggerboard	159	20.05	39.22	7.10	1.0	0.0	18
T Foil	160	20.05	75.66	7.16	2.0	0.0	18
	161	20.05	124.44	8.48	3.0	0.0	18
	162	20.05	162.64	9.67	4.0	0.0	18
Fresh Water	163	20.05	207.85	11.45	5.0	0.0	18
T =63.0 F	164	20.05	274.70	15.93	6.0	0.0	18
	165	20.05	-31.01	7.82	-1.0	0.0	18
	166	20.05	-60.95	8.48	-2.0	0.0	18
	167	20.05	-100.11	9.68	-3.0	0.0	18
	168	20.04	161.74	9.39	4.0	0.0	18
	169	20.05	165.47	10.18	4.0	0.0	24
	170	20.05	154.06	8.66	4.0	0.0	12
	171	20.05	139.45	8.00	4.0	0.0	6
	172	20.04	164.33	9.35	4.0	0.0	12
	173	20.05	151.35	8.42	4.0	0.0	6
	174	20.02	162.54	9.27	4.0	0.0	18
	175	20.03	181.21	10.41	4.0	1.0	18
	176	20.03	89.27	7.95	1.0	3.0	18
	177	20.03	234.67	12.94	1.0	10.0	18
	178	20.03	178.92	10.52	1.0	7.5	18
	179	20.04	173.90	10.20	2.0	5.0	18
	180	20.04	182.53	10.69	2.0	5.5	18
	181	20.04	174.85	10.14	3.0	3.0	18
	182	20.04	180.70	10.44	3.0	3.3	18
	183	20.04	163.12	10.03	5.0	-1.1	18
	184	20.05	182.38	10.29	5.0	-0.4	18
	185	20.05	187.25	10.99	6.0	-2.9	18
	186	20.05	173.29	10.33	6.0	-3.5	18
	187	20.05	176.59	10.56	6.0	-3.2	18
	188	20.05	192.50	11.57	7.0	-5.0	18
	189	20.05	179.15	10.94	7.0	-5.5	18
	190	20.05	182.08	11.01	0.0	9.5	18
	191	20.05	197.66	10.86	5.0	-0.5	18
	192	20.05	198.67	11.18	5.0	-0.5	18
	193	20.05	191.93	11.21	5.0	-0.5	18
	194	20.05	184.19	10.70	5.0	-0.5	18

Table A1 – Raw Data for Hungry Beaver Faired Struts and Foils

Geometry	Data File	Velo (fps)	Lift (lb)	Drag (lb)	Foil Pitch Angle (deg)	Flap Angle (deg)	Depth (in)
Vendor1	71	20.05	72.27	7.10	0.0	0.0	18
Daggerboard	72	20.05	113.54	7.85	1.0	0.0	18
T Foil	73	20.05	149.00	8.48	2.0	0.0	18
	74	20.05	224.01	11.92	3.9 (est. after foil slipped)	0.0	18
	75	20.05	33.73	6.85	-1	0.0	18
Fresh Water	76	20.05	13.83	7.32	-2	0.0	18
T = 59.2 F	77	20.05	-34.04	6.83	-3	0.0	18
	78	20.05	-69.78	8.30	-4	0.0	18
	79	20.05	6.95	7.52	-2	0.0	18
	80	20.05	6.93	6.51	-2	0.0	18
	81	20.05	110.50	8.29	-2	5.0	18
	82	20.05	178.18	10.95	-2	8.5	18
	83	20.05	146.55	8.97	-1	5.0	18
	84	20.05	176.46	10.61	-1	6.5	18
	85	20.05	168.53	10.10	0	4.5	18
	86	20.05	176.15	10.27	0	5.0	18
	88	20.05	183.27	10.36	1	3.5	18
	89	20.05	196.42	10.17	2	2.3	18
	90	20.05	179.83	9.88	2	1.5	18
	91	20.05	172.94	9.41	3	-0.5	18
	92	20.05	171.00	10.11	4	-2.5	18
	93	20.05	179.54	10.49	4	-2.0	18
	95	20.05	181.77	10.19	5	-4.0	18
	96	20.05	174.50	9.68	6	-6.0	18
	97	20.05	181.24	10.33	6	-5.5	18
Vendor1	53	20.03		1.43			12
Daggerboard	54	20.04		1.64			12
Vertical	55	10.02		0.50			12
Strut	55	15.03		0.94			12
	56	25.05		2.33			12
	57	30.05		3.30			12
Fresh Water	58	20.04		1.75			12
T = 59.0 F	59	20.05		1.53			12
	60	20.04		2.88			24
	61	10.02		0.86			24
	61	15.05		1.66			24
	62	25.07		4.14			24
	63	30.07		5.99			24
	64	20.06		2.70			24
	65	20.05		2.75	Strut Raked Fwd 8 deg		24
	66	20.05		2.77	Strut Raked Fwd 8 deg		24
	67	20.05		2.77	Strut Raked Fwd 8 deg		24
	68	20.05		2.57	Strut Raked Fwd 8 deg		24
	69	20.05		2.57	Strut Raked Fwd 8 deg		24
Vendor1	110	20.05	48.10	5.12	-0.65		18
Rudder	111	20.05	47.76	5.12	-0.65		18
T Foil	112	20.05	69.23	5.35	0.35		18
	113	20.05	100.44	6.01	1.35		18
	114	20.05	128.35	6.69	2.35		18
Fresh Water	115	20.05	154.24	7.94	3.35		18
T = 61.2 F	116	20.05	15.80	4.92	-1.65		18
	117	20.05	-7.19	5.08	-2.65		18
	118	20.05	-37.17	5.40	-3.65		18
	119	20.04	-66.36	6.32	-4.65		18
	120	20.05	67.52	5.77	0.35		24
	121	20.05	72.93	4.87	0.35		12
	122	20.05	66.88	4.00	0.35		6
Vendor1	98	10.02		0.46			12
Rudder	99	10.02		0.46			12
Strut	100	15.04		0.94			12
	101	20.04		1.67			12
	102	25.05		2.39			12
Fresh Water	103	30.06		3.55			12
T = 61.2 F	104	20.05		1.72			12
	105	10.02		0.82			24
	105	15.04		1.62			24
	106	20.05		2.80			24
	107	25.05		4.26			24
	108	30.06		5.83			24
	109	25.06		4.17			24

Table A2 – Raw data for Vendor1 Struts and Foils

Geometry	Data File	Velo (fps)	Lift (lb)	Drag (lb)	Foil Pitch Angle (deg)	Flap Angle (deg)	Depth (in)
Vendor2	196	10.04	0.07	0.56			12
Daggerboard	196	15.06	-0.38	1.15			12
Vertical	197	20.08	-1.34	2.12			12
Strut	198	20.08	-1.46	2.07			12
	199	25.09	-1.09	3.11			12
	200	30.10	-1.27	4.28			12
	201	10.02	-0.24	1.14			24
Fresh Water	201	15.06	-0.16	2.17			24
T = 67.5 F	203	20.08	0.23	3.65			24
	204	25.09	0.38	5.59			24
	205	30.11	2.03	7.85			24
	206	10.02	-0.12	1.16			24
	206	20.08	0.07	3.58			24
	207	20.08	-0.24	2.84			18
	208	20.08	0.06	2.89			18
Vendor2	210	20.08	-5.65	7.22	0	0.0	18
Daggerboard	211	20.08	30.09	7.52	1	0.0	18
T Foil	212	20.07	63.46	7.84	2	0.0	18
	213	20.06	97.91	7.73	3	0.0	18
	214	20.06	141.09	8.64	4	0.0	18
Fresh Water	215	20.07	185.99	10.26	5.6 (est. after foil slipped)	0.0	18
T = 67.5 F	216	20.07	203.04	10.86	6	0.0	18
	217	20.07	199.76	10.55	6	0.0	18
	218	20.08	234.09	12.53	7	0.0	18
	219	20.06	161.94	9.16	5	0.0	18
	220	20.07	61.14	6.88	2	0.0	18
	221	20.08	23.97	7.40	1	0.0	18
	222	20.07	-5.64	8.09	0	0.0	18
	223	20.07	-47.28	7.52	-1	0.0	18
	224	20.07	-75.51	7.63	-2	0.0	18
	225	20.07	120.92	8.17	4	0.0	18
	226	20.07	188.11	10.58	4	5.0	18
	227	20.06	183.79	10.43	4	4.5	18
	228	20.08	181.85	10.44	4	4.3	18
	229	20.07	154.22	10.25	2	7.0	18
	230	20.07	182.54	11.21	2	9.0	18
	231	20.06	174.77	11.47	0	13.5	18
	232	20.07	181.27	11.52	0	14.0	18
	233	20.07	183.67	10.27	6	-1.0	18
	234	20.07	180.50	9.96	6	-1.3	18
	235	20.07	192.01	10.38	8	-7.0	18
	236	20.06	186.53	10.27	8	-8.0	18
	237	20.07	178.80	10.19	8	-9.0	18
	238	20.08	144.43	8.60	5	-1.25	18
	239	20.07	174.68	9.96	5	1.25	18
	240	20.07	181.57	9.65	5	1.75	18
	241	20.06	176.55	10.01	5	1.75	18
	242	20.08	189.72	11.23	3	7.0	18
	243	20.06	183.06	10.72	3	6.5	18
	244	20.07	175.05	9.48	7	-5.0	18
	245	20.08	181.12	9.71	7	-4.5	18
	246	20.07	180.59	9.92	7	-4.5	18
	247	20.07	186.39	9.86	6	-1.3	18
	248	20.08	183.30	9.93	6	-1.8	18
	249	20.08	184.74	10.53	4	4.2	18
	250	20.07	179.62	10.47	4	3.7	18
	251	20.08	171.99	9.87	8	-9.0	18
	252	20.07	181.83	10.12	8	-8.2	18
	253	20.07	178.90	9.88	6	-1.8	18
	254	20.07	175.59	9.19	6	-1.8	12
	255	20.07	163.45	8.10	6	-1.8	6
	256	20.07	180.60	10.29	6	-1.8	24
Vendor2	257	20.03	34.77	5.34	-0.4		18
Rudder	258	20.03	35.77	5.48	-0.4		18
T Foil	259	20.03	56.57	5.61	0.6		18
	260	20.03	88.49	6.46	1.6		18
	261	20.03	114.97	7.44	2.6		18
Fresh Water	262	20.03	142.05	8.26	3.6		18
T = 65.8 F	263	20.03	6.44	5.42	-1.4		18
	264	20.02	-18.89	5.96	-2.4		18
	265	20.02	-47.47	6.79	-3.4		18
	266	20.02	56.27	6.62	0.6		24
	267	20.03	57.37	5.73	0.6		18
	268	20.03	55.61	5.13	0.6		12
	269	20.03	52.44	4.47	0.6		6

Table A3 – Raw data for Vendor2 Struts and Foils

Geometry	Data File	Velo (fps)	Lift (lb)	Drag (lb)	Foil Pitch Angle (deg)	Flap Angle (deg)	Depth (in)
JZ	43	20.05	-0.77	1.32			12
Vertical	44	10.01	-0.11	0.52			12
Strut	44	15.04	-0.44	0.86			12
	45	25.06	-0.95	2.08			12
	46	30.06	-1.00	2.81			12
	47	20.05	-0.65	2.46			24
Fresh Water	48	20.05	0.36	2.27			24
T = 59.0 F	49	10.02	-0.04	0.77			24
	49	15.04	-0.28	1.48			24
	50	25.06	-0.42	3.46			24
	51	30.06	-0.56	4.81			24
	52	20.05	0.01	2.39			24

Table A4 – Raw Data for JZ Vertical Strut

Configuration	Data File	Velo (fps)	Drag (lb)	Side Force (lb)
Upright w/Driver	38	20.05	3.934	4.871
	39	20.05	3.675	4.915
	40	20.05	3.790	5.054
	41	20.05	3.862	4.862
	42	20.06	3.932	4.981
		average =	3.839	4.937
		stdev =	0.109	0.081
15 Deg Heel w/Driver	43	20.05	2.965	4.435
	45	20.05	2.948	4.470
	46	20.05	3.315	4.641
	47	20.05	3.164	4.498
	48	20.05	3.246	4.983
		average =	3.127	4.605
		stdev =	0.165	0.225
30 Deg Heel w/Driver	49	20.05	2.994	5.400
	50	20.04	3.013	5.529
	51	20.05	2.932	5.604
	52	20.06	2.921	5.394
	53	20.05	3.078	5.636
		average =	2.988	5.513
		stdev =	0.064	0.113
30 Deg Heel w/o Driver	54	20.05	1.633	5.142
	55	20.05	1.890	5.581
	56	20.05	1.654	5.325
	57	20.04	1.780	5.274
	58	20.04	1.676	5.081
		average =	1.727	5.281
		stdev =	0.107	0.195

Table A5 – Raw data for Aerodynamic Tests